THE ASTROPHYSICAL JOURNAL, 558:553–560, 2001 September 10

SEARCHING FOR THE PHYSICAL DRIVERS OF THE EIGENVECTOR 1 CORRELATION SPACE

P. MARZIANI,[1] J. W. SULENTIC,[2] T. ZWITTER,[3] D. DULTZIN-HACYAN,[4] AND M. CALVANI[1]

Received 2000 December 14; accepted 2001 May 10

ABSTRACT

We recently discussed an Eigenvector 1 (E1) parameter space that provides optimal discrimination between the principal classes of broad-line active galactic nuclei (AGNs). In this paper we begin a search for the most important physical parameters that are likely to govern correlations and data point distribution in E1 space. We focus on the principal optical parameter plane involving the width of the Hβ broad component [FWHM(Hβ_{BC})] and the equivalent width ratio between the Fe II blend at 4570 Å and Hβ_{BC}. We show that the observed correlation for radio-quiet sources can be accounted for if it is primarily driven by the ratio of AGN luminosity to black hole mass ($L/M \propto$ Eddington ratio) convolved with source orientation. L/M apparently drives the radio-quiet correlation only for FWHM(Hβ) $\lesssim 4000$ km s^{-1}, which includes narrow-line Seyfert 1 galaxies and can be said to define an AGN "main sequence." Source orientation plays an increasingly important role as FWHM(Hβ_{BC}) increases. We also argue that AGNs lying outside the radio-quiet main sequence, and specifically those with optical Fe II much stronger than expected for a given FWHM(Hβ_{BC}), may all be broad absorption line QSOs.

Subject headings: line: formation — line: profiles — quasars: emission lines — quasars: general

1. INTRODUCTION

We have recently identified a correlation space for broad-line active galactic nuclei (AGNs) involving (1) Balmer line width (FWHM Hβ_{BC}), (2) relative strength of optical Fe II and Hβ emission lines [the equivalent width ratio of Fe II$_{opt}$ emission in the range 4435–4685 Å and the broad component of Hβ: W(Fe II λ4570)/W(Hβ_{BC}) = $R_{Fe\,II}$], (3) soft X-ray photon index Γ_{soft}, and (4) C IV λ1549 broad-line profile centroid shift (Sulentic, Marziani, & Dultzin-Hacyan 2000a; Sulentic et al. 2000b). In simplest terms, the parameters can be said to measure (1) the broad-line region (BLR) velocity dispersion, (2) the relative strengths of low-ionization lines that are thought to arise in the same structure, (3) the strength of a (thermal) soft X-ray photon excess, and (4) the amplitude of systematic radial motions in the high-ionization gas. We call this parameter space "Eigenvector 1" (E1), reflecting its partial origin in a principal component analysis of the low-redshift ($z \lesssim 0.5$) part of the Palomar-Green quasar sample (Boroson & Green 1992, hereafter BG92). E1 allows us to discriminate between most AGN classes that show broad emission lines (Sulentic et al. 2000a, 2000b).

E1 separates the majority of radio-quiet (RQ) sources from radio-loud (RL) AGNs. The E1 parameter-space distribution also suggests the possible existence of two RQ classes. Population A has FWHM(Hβ_{BC}) $\lesssim 4000$ km s^{-1}, average E1 parameter values of $R_{Fe\,II} \approx 0.7$ and $\Gamma_{soft} \approx 2.8$, and a C IV λ1549 centroid (blue-) shift of approximately -800 km s^{-1}. Population B includes all of the remaining RQ AGNs, with FWHM(Hβ_{BC}) $\gtrsim 4000$ km s^{-1}, average E1 parameter values of $R_{Fe\,II} \approx 0.4$ and $\Gamma_{soft} \approx 2.3$, and a C IV λ1549 centroid shift of ~ 0 km s^{-1}. See Sulentic et al. (2000b) for sample variance and other details. RL and RQ population B sources occupy a similar parameter domain in E1 and show a large number of other observational similarities (Sulentic et al. 2000b).

After reviewing the occupancy of the optical E1 parameter plane [FWHM(Hβ_{BC}) vs. $R_{Fe\,II}$] and defining a "main sequence" for RQ population A, we show that the mean ionization level of the broad lines decreases as one goes from RQ population B to population A sources (§ 2.2). In § 4, we show how this result and the occupancy of the parameter plane can be explained in terms of different values of the Eddington ratio (analyzed in § 3.2) convolved with the effect of source orientation (discussed in §§ 3.1 and 3.2). We also consider potentially important outlier sources in §§ 2.1 and 6.1.

2. RELEVANT TRENDS

2.1. *Definition of Main Sequence and Outliers*

Population A sources show a clear and significant correlation among the E1 parameters, while RQ population B and RL sources show a larger scatter with no obvious correlation. RQ population B sources occupy the same E1 parameter domain as, especially, flat-spectrum (core dominated) RL sources (see Table 2 in Sulentic et al. 2000b). It is, however, important to recognize that uncertainties are larger for most measures of RL and RQ population B sources. Limited signal-to-noise ratio (S/N) and line blending limit the accuracy of Fe II$_{opt}$ equivalent width measurements for sources with W(Fe II λ4570) $\lesssim 20$ Å ($R_{Fe\,II} \lesssim 0.2$). That is why we cannot rule out the possibility that the RQ–population A correlation extends into the RQ population B domain. At any rate, the RL sources are preferentially found in the same E1 domain as RQ population B and are rarely found in the domain of population A. The concepts of an RQ population A–population B difference and of an RQ population B–RL similarity were motivated by the optical parameters, but they are reinforced by X-ray Γ_{soft} and UV C IV λ1549 shift measures. These differences and similarities

[1] Osservatorio Astronomico di Padova, vicolo dell'Osservatorio 5, I-35122 Padova, Italy; marziani@pd.astro.it, calvani@pd.astr.it.

[2] Department of Physics and Astronomy, University of Alabama, Box 870324, Tuscaloosa, AL 35487; giacomo@merlot.astr.ua.edu.

[3] Department of Physics, Univerza Ljubljani, Jadranska 19, SI-1000 Ljubljana, Slovenia; tomaz.zwitter@uni-lj.si.

[4] Instituto de Astronomía, Universidad Nacional Autónoma de México, Apdo. Postal 70-264, 04510 México, D.F.; deborah@astroscu.unam.mx.

are true irrespective of the reality of a parameter-space break between populations A and B (Sulentic et al. 2000b).

Figure 1 presents a schematic view of source occupancy in the FWHM($H\beta_{BC}$) versus $R_{Fe\,II}$ parameter plane. We show correlation trends for (1) our sample (Sulentic et al. 2000b), (2) two radio-loud samples (Brotherton 1996; Corbin 1997), and (3) a soft X-ray–selected sample (Grupe et al. 1999). The solid lines representing samples 1 and 3 connect average values for sources in FWHM($H\beta_{BC}$) ranges 0–2000, 2000–4000, and $\gtrsim$4000 km s^{-1}, respectively. All samples show the same general trends, with broad-line, Fe II$_{opt}$ weak, RQ population B and RL sources displaced toward the upper left, and narrow-line, Fe II$_{opt}$ strong, RQ population A sources toward the lower right. These lines indicate a tendency for AGNs to lie along a main sequence. In addition to some prototype sources, we show data points for Fe II$_{opt}$ strong (far-IR bright) quasars (Lipari, Terlevich, & Macchetto 1993). The Lipari et al. (1993) sources are shown as a single point representing their average FWHM($H\beta_{BC}$) and $R_{Fe\,II}$, with the exception of two objects, IRAS 0759+651 and Mrk 231, which are reported individually in Figure 1. We also identify all known broad absorption line (BAL) QSOs with absorption W(C IV λ1549) $\lesssim -9$ Å from the Sulentic et al. (2000b) and Lipari et al. (1993) samples. For PG quasars, data on absorption W(C IV λ1549) were obtained from Brandt, Laor, & Wills (2000) except for PG 1351+234, for which we measured the C IV λ1549 absorption on the *International Ultraviolet Explorer* spectrum SWP54205.

We see that I Zw 1 (and other narrow-line Seyfert 1 galaxies), as well as several (low z) BAL QSOs, are located toward the high-$R_{Fe\,II}$ end of the main sequence. One could infer from Figure 1 that the main sequence may extend from the broadest double-peaked RL sources to the narrowest and Fe II$_{opt}$ strongest sources (such as PHL 1092). It is not yet clear if these extrema should be considered outliers or extensions of the correlation found for the bulk of RQ population A sources studied so far (see also § 6). We can identify one clear class of outliers: sources occupying the upper right quadrant of the E1 plane (Fig. 1), which all turn

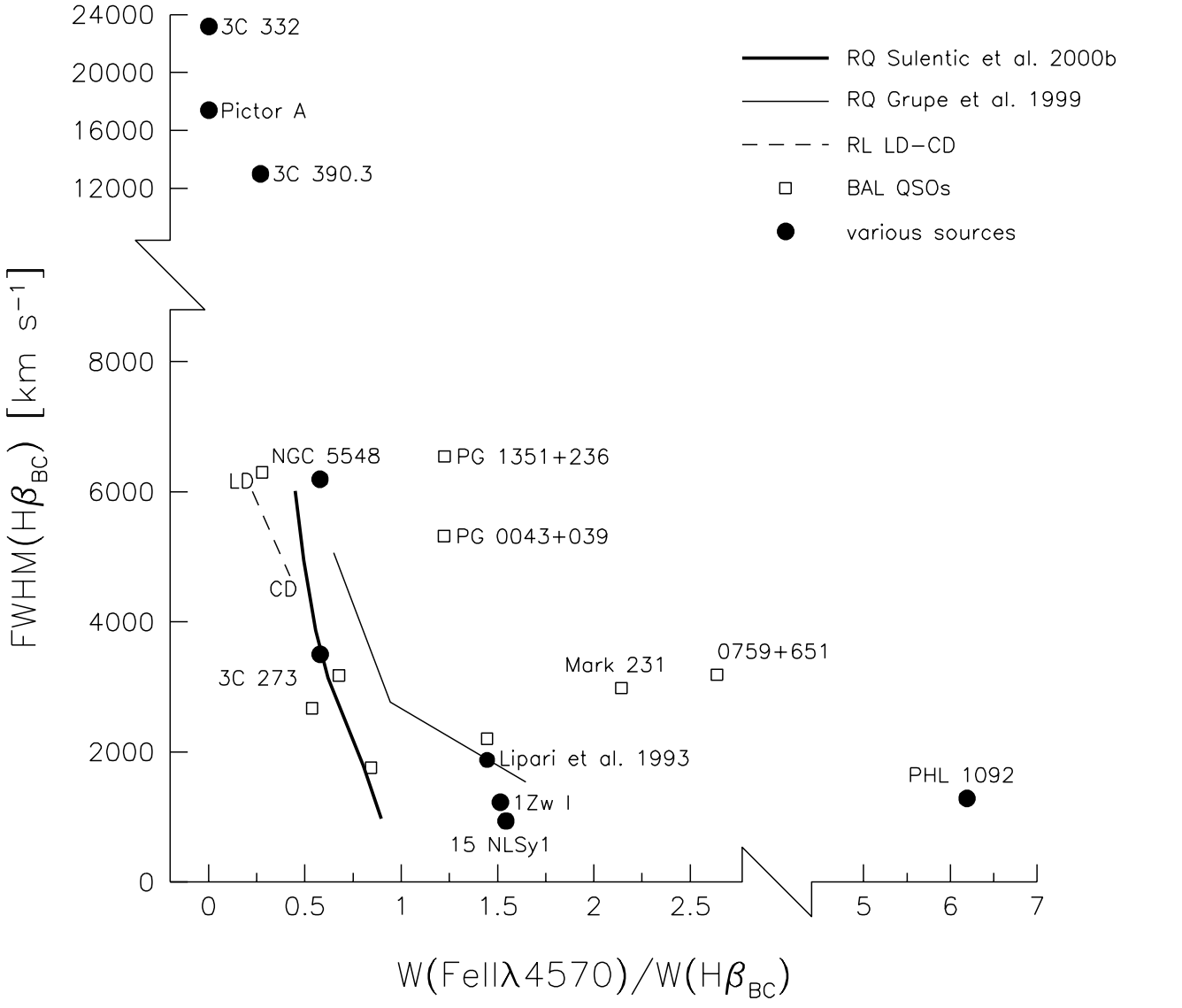

FIG. 1.—FWHM ($H\beta_{BC}$) vs. $R_{Fe\,II}$ parameter plane. The two solid lines mark the average positions of the sample of Grupe et al. (1999) and Sulentic et al. (2000b). The dashed line traces the average loci of core-dominated (CD) and lobe-dominated (LD) RL AGNs. Squares identify BAL QSOs. The five unlabeled objects are PKS 1004+130, PG 1411+442, PG 2112+059, PG 1011+054, and PG 1700+518 (in order of increasing $R_{Fe\,II}$). Other relevant sources (see §2.1) are also plotted. The broken scale allows for the inclusion of three wide-separation double-peaked RL AGNs, as well as PHL 1092.

TABLE 1

EMISSION-LINE MEAN PARAMETER VALUES FOR RADIO-QUIET AGN POPULATIONS

AGN Population	$W(H\beta_{BC})$ (Å)	W(Fe II λ4570) (Å)	$R_{Fe\,II}$	I(Si III] λ1892)/I(C III] λ1909)	W(C IV λ1549) (Å)
NLSy1	72 ± 28	54 ± 17	0.8 ± 0.3	0.53 ± 0.16	41 ± 19
Population A.....	95 ± 39	60 ± 16	0.5 ± 0.3	0.43 ± 0.19	50 ± 25
Population B.....	104 ± 34	31 ± 17	0.3 ± 0.1	0.23 ± 0.11	107 ± 85

out to be BAL QSOs. These are sources with FWHM($H\beta_{BC}$) $\gtrsim$ 3000 km s^{-1} and $R_{Fe\,II} \gtrsim 1$. In general, sources with $R_{Fe\,II} \gg [\mathrm{FWHM}(H\beta_{BC})/(2500\ \mathrm{km\ s^{-1}})]^{-1.4}$ (which approximately defines the upper boundary to the main sequence of Sulentic et al. 2000a) are sources with Fe II$_{opt}$ in excess of the mean value expected for a given FWHM($H\beta_{BC}$). They will be briefly considered in § 6.1.

2.2. *An Ionization Decrease from Population B to Population A*

Table 1 shows relevant mean parameter values for RQ population A and B sources, as well as for the extreme population A narrow-line Seyfert 1 (NLSy1) sources. All averages and sample standard deviations are from Sulentic et al. (2000b) except for I(Si III] λ1892)/I(C III] λ1909), which comes from *Hubble Space Telescope* data (Laor et al. 1994, 1995; Wills et al. 1999). The decrease in equivalent width of C IV λ1549 (our representative high-ionization line) along with an increase in W(Fe II λ4570) (low-ionization emission) suggests a systematic decrease in ionization level from RQ population B to population A. We interpret the data in Table 1 by considering the behavior of I(Si III] λ1892)/I(C III] λ1909), W(C IV λ1549), and $W(H\beta_{BC})$ as a function of the ionization parameter (U) and electron density n_e. We compare the observed values with a grid of CLOUDY computations for AGN broad-line emission (Korista et al. 1997). The models assumed a total column density $N_C \sim 10^{23}$ cm^{-2} and a standard AGN continuum (model 3-23 in Korista et al. 1997). Figure 2 shows that all trends passing from population B toward population A consistently suggest a decrease in U and an increase in n_e (from $\log U \sim -1$ to -1.5, $\log n_e \sim 9.5$, the canonical value from AGN photoionization models, to $\log U \sim -2$ to -2.5, $\log n_e \sim 11.5$). Notably, the density-sensitive line ratio I(Si III] λ1892)/I(C III] λ1909), almost independent of U for $\log U \lesssim -0.5$, indicates that $\log n_e \sim 10.5$–11 toward the NLSy1 domain.

These considerations quantify a general trend that is *very appreciable* in the spectra of AGNs with different Balmer line widths (see Fig. 2 of Sulentic et al. 2000a) and which has been systematically ignored in photoionization computations. It is probably the origin of our inability to explain some line ratios in quasar spectra (Sulentic et al. 2000b) and is obviously a zeroth-order result. Our earlier comparison of C IV $\lambda 1549_{BC}$ and $H\beta_{BC}$ properties motivated us to suggest that high- and low-ionization lines are not emitted in the same region, at least in population A sources (Marziani et al. 1996; Dultzin-Hacyan, Marziani, & Sulentic 2000).

3. THE MAIN PHYSICAL PARAMETERS

3.1. *The Role of Orientation in E1*

Why is orientation important, and why, at the same time, can it not account for all of the phenomenology? Important evidence in favor of orientation effects in RQ AGNs involves $H\beta_{BC}$–C IV$_{BC}$ λ1549 profile comparisons (Marziani et al. 1996; Sulentic et al. 2000b). Some NLSy1 sources, such as I Zw 1, show a C IV$_{BC}$ λ1549 profile that is almost completely blueshifted relative to a very narrow $H\beta_{BC}$. This robust observational result is easily explained in terms of (1) a high-ionization wind emitting C IV$_{BC}$ λ1549, and (2) an optically thick disk emitting $H\beta_{BC}$. The disk will obscure the opposite (receding) side of the high-ionization outflow (Marziani et al. 1996). Not all NLSy1's show large-amplitude C IV λ1549 blueshifts, but the currently observed range is from 0 to -5000 km s^{-1}. NLSy1's also show low W(C IV λ1549) (Rodriguez-Pascual, Mas-Hesse, & Santos-Lleo 1997). The rarity of large-amplitude C IV λ1549 blueshifts points toward a role for orientation, since C IV λ1549 shifts are expected to be strongly orientation dependent in a disk + wind scenario.

In principle, it is possible to ascribe low $W(H\beta_{BC})$, W(C IV λ1549), and W([O III] λ5007) to an orientation-dependent "blue bump" that amplifies the UV/optical continua and whose contribution to the continua increases with decreasing inclination (Marziani et al. 1996). However, this assumption is rather ad hoc and cannot easily account for the increase of $R_{Fe\,II}$ in sources with narrower FWHM($H\beta_{BC}$). In that scenario, $R_{Fe\,II}$ should remain constant, because $H\beta_{BC}$ and Fe II$_{opt}$ would be similarly affected by the amplified continuum unless $H\beta_{BC}$ and Fe II$_{opt}$ are both, but differently, anisotropic (Marziani et al. 1996). We remark that the observed $R_{Fe\,II}$ increase appears to be mainly due to a decrease in $W(H\beta_{BC})$ toward the NLSy1 domain. This has been interpreted as the effect of collisional suppression of $H\beta$ (Gaskell 1985), implying an increase in electron density. The correlation between the n_e-sensitive I(Si III] λ1892)/I(C III] λ1909) ratio and FWHM($H\beta_{BC}$) also cannot be explained in terms of orientation. Physical conditions must change significantly along the AGN main sequence.

Further difficulties for an orientation-only hypothesis may involve the range of [O III] $\lambda\lambda$4959, 5007 luminosity observed among PG quasars (BG92). We suggest that this issue needs reconsideration also because the [O III] $\lambda\lambda$4959, 5007 emitting region in several Seyfert galaxies shows a bipolar structure (Falcke, Wilson, & Simpson 1998), a result that suggests a strong orientation dependence.

3.2. *The Eddington Ratio: A Parameter Affecting BLR Physical Conditions*

E1 shows us that the diversity of AGN properties can be organized on the basis of a set of parameters involving Γ_{soft}, FWHM($H\beta_{BC}$), $R_{Fe\,II}$, and C IV λ1549 line shift. Apart from the reasons outlined above, it is reasonable to infer that orientation alone would be unlikely to account for the E1 correlations, because we would expect to find an overlapping domain for *all* RQ and RL AGNs. A distinct RL

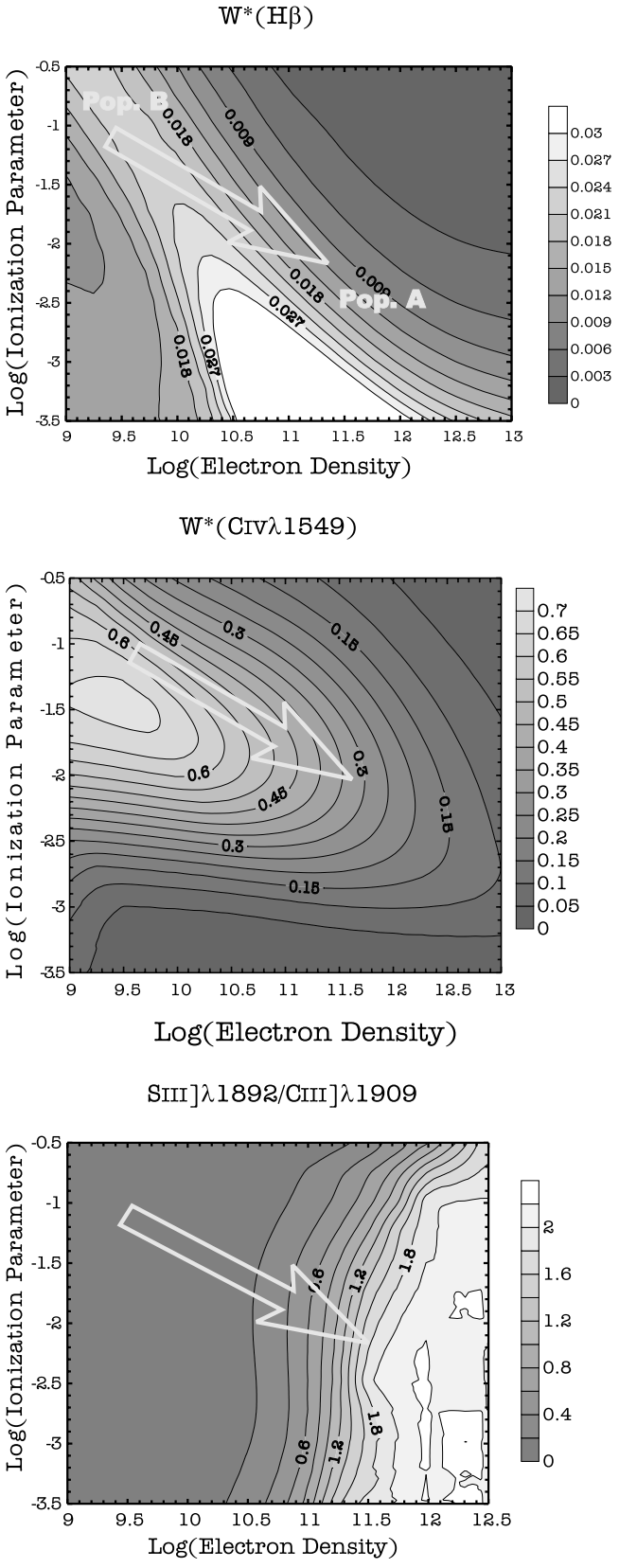

FIG. 2.—Behavior of the ratio I(Si III] λ1892)/I(C III] λ1909), of normalized W(C IV λ1549), and of normalized W(Hβ) as a function of electron density n_e and ionization parameter, computed with CLOUDY by Korista et al. (1997). Arrow tails are placed roughly at the value of (n_e, U) expected for population B sources, and arrow heads at that for population A. Equivalent width normalization is by continuum at 912 Å (see Korista et al. 1997 for further details).

sequence, if it exists, is apparently displaced from the RQ one. E1 suggests that it begins near FWHM($H\beta_{BC}$) $\sim$ 4000 km s^{-1} (Sulentic et al. 2000a, 2000b). Our BG92-dominated sample suggests that RQ sources become rare above FWHM($H\beta_{BC}$) $\sim$ 6000 km s^{-1}, while RL sources are common from 4000 to, at least, 8000 km s^{-1}. Support for an RQ-RL displacement comes from the detection of a strong Hα line in BL Lacertae objects with FWHM(Hα) $\sim$ 4000 km s^{-1} (Corbett et al. 2000), which should be a nearly pole-on RL source. The presence of the soft X-ray excess as one of the principal correlates in E1 suggests that the Eddington ratio (i.e., the ratio L/M) may be the most important physical parameter driving E1, as well as the main factor accounting for the RQ and RL sequence displacement (BG92; Pounds, Done, & Osborne 1995; Boller, Brandt, & Fink 1996; Sulentic et al. 2000a).

3.3. *A Correlation between* FWHM($H\beta_{BC}$) *and* L/M*?*

We often refer to the L/M ratio rather than the Eddington ratio (the ratio between the bolometric and Eddington luminosities, equal to the dimensionless accretion rate $\dot{m} \propto L/M$) because we rely, in this context, on independent observational measurements for both L and M. X-ray variability determination of M for a few AGNs (Czerny et al. 2001) suggests an anticorrelation between L/M and FWHM($H\beta_{BC}$). Figure 3 shows the best current observational evidence for the anticorrelation between dimensionless accretion rate and FWHM($H\beta_{BC}$). It involves the sources with the most accurate reverberation and/or X-ray variability–based black hole mass determinations. Sources such as NGC 4051 and NGC 4151 show a transient broad-line component, which at some epochs is completely absent

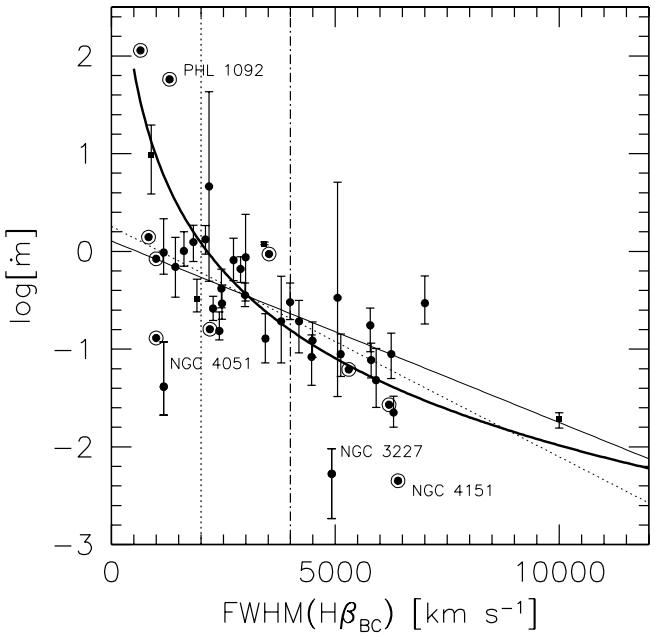

FIG. 3.—Relationship between dimensionless accretion rate and FWHM ($H\beta_{BC}$). Filled circles and squares are RQ and RL AGNs, respectively, with reverberation-mapping mass estimates from Kaspi et al. (2000). Ringed filled circles label AGNs with an X-ray variability mass determination (Czerny et al. 2001). The heavy line marks the prediction of a disk + wind model (Nicastro 2000). The thin line is the best fit, employing robust techniques for all data points of Kaspi et al. (2000); the thin dotted line represents the same with the exclusion of radio-loud AGNs. The vertical lines mark the boundaries of NLSy1's (*dotted line*) and population A nuclei (*dot-dashed line*).

in unpolarized light (see, e.g., Ulrich, Maraschi, & Urry 1997 and references therein). FWHM($H\beta_{BC}$) and X-ray properties for such sources may not allow a reliable mass estimate that is comparable to AGNs showing a more typical variability pattern. At the other extreme, the two highest $\dot{m}$ radiators, PHL 1092 and IRAS 13224−3809, show extreme optical properties (see § 6 for a possible interpretation). The Czerny et al. (2001) data set is obviously biased toward objects that show large-amplitude X-ray variability. Only six sources remain in the X-ray sample if we omit them, which is too few for a reliable determination of the correlation coefficient. The results shown in Figure 3 are suggestive, with the X-ray–based points showing a correlation at a 2 σ confidence level. If only the six sources are considered, Pearson's correlation coefficient $r_P \approx -0.85$, with a probability $P \approx 0.04$ that uncorrelated points could give rise to the computed r_P. If all data points are taken into account, $r_P \approx -0.75$ ($P \approx 0.02$).

Other approaches favor a strong correlation between $\dot{m}$ and FWHM($H\beta_{BC}$). Modeling of a radiation pressure–driven wind (Nicastro 2000; Witt, Czerny, & Życki 1997) predicts the relationship between $\dot{m}$ and FWHM($H\beta_{BC}$) (Fig. 3, *thick line*). A rather strong correlation between L/M and FWHM($H\beta_{BC}$) also emerges using masses derived from reverberation mapping (Kaspi et al. 2000; *filled circles and squares*). If all RQ and RL objects are considered except the outliers NGC 3227 (another transient $H\beta_{BC}$ object) and NGC 4051, the correlation coefficient is $r_P \approx -0.75$ ($P \approx 2 \times 10^{-4}$). We obtain the following functional relationship by a robust fitting technique (see, e.g., Press et al. 1992, p. 694):

$$(\lambda L_\lambda/M)_\odot \approx 6.2 \times 10^3 \mathrm{FWHM}_{1000}(H\beta_{BC})^{-2}\,, \qquad (1)$$

where L_λ is the specific luminosity at $\approx$5000 Å and FWHM($H\beta_{BC}$) is expressed in units of 1000 km s^{-1}. In order to transform to $\dot{m}$, we assume a constant bolometric correction of approximately −2.5, appropriate for the typical AGN continuum as parameterized by Mathews & Ferland (1987). The $\dot{m}$-FWHM($H\beta_{BC}$) best fit is shown in Figure 3 as a thin solid line.

An FWHM($H\beta_{BC}$)-L/M correlation in the case of reverberation masses is not surprising, since it results in part from circular arguments [i.e., FWHM($H\beta_{BC}$) is used to compute M from reverberation-mapping data]. Monte Carlo simulations were carried out assuming (1) that distance r, FWHM($H\beta_{BC}$), and luminosity are randomly distributed and uncorrelated in the observed ranges, and (2) that M is related to the velocity dispersion by the virial relationship $M \propto rv^2$. Observational errors for log $\dot{m}$ were assumed to contribute a Gaussian scatter with $\sigma \approx 0.15$. In approximately 4000 random trials, we found a probability $P \lesssim 0.05$ that a correlation coefficient as large as 0.75 would be obtained. In order to fully circumvent the circularity issue, we also assumed that FHWM($H\beta_{BC}$) does not correlate strongly with either L or M separately (as noted also by Sulentic et al. 2000a). Optical luminosity appears to be an orthogonal variable with respect to the E1 parameters (in BG92 it is part of their Eigenvector 2). Mass and FWHM($H\beta_{BC}$) have $r_P \approx 0.48$. If we simulate data points for which (1) the correlation between FWHM($H\beta_{BC}$) and M falls in the range $0.43 \lesssim r_P \lesssim 0.53$ and (2) mass and luminosity are not correlated, we obtain a negligible probability that an $r_P \approx 0.75$ correlation between FWHM($H\beta_{BC}$) and log $\dot{m}$ could occur randomly.

We conclude that the circularity inherent in the mass computation cannot fully explain the strength of the observed L/M versus FWHM($H\beta_{BC}$) correlation for reverberation masses. This provides much-needed support for a physical relationship between L/M and FWHM($H\beta_{BC}$). Given the caveats outlined above [i.e., small numbers of X-ray–determined masses and M(FWHM) dependence in optical reverberation masses], an independent verification of any $\dot{m}$-FWHM($H\beta_{BC}$) relationship would be best derived from X-ray variability (V. Braito & P. Marziani, in preparation). In the present study, we assume that equation (1) describes the appropriate relation.

Differences between the disk + wind model expectation and the linear fit described by equation (1) are appreciable for FWHM($H\beta_{BC}$) $\lesssim$ 1500 km s^{-1} (Fig. 3). The disk + wind model predicts an average difference of more than 1 order of magnitude between NLSy1 and other population A sources. The assumption of constant $\dot{m}$ for all population A yields a lower normalized χ^2_ν ($\approx$3.2) than the disk + wind fit ($\chi^2_\nu \approx 4.3$; see also § 6 for possible interpretations).

4. WHY DOES IONIZATION LEVEL DECREASE WITH INCREASING L/M?

The ionization parameter can be defined as

$$U = \frac{Q(\mathrm{H})}{4\pi r^2 n_e c}\,, \qquad (2)$$

where Q(H) is the number of hydrogen-ionizing photons and r is the distance of the BLR from the central continuum source. U can be rewritten in terms of L/M and M if we assume the following:

1. $Q(\mathrm{H}) \approx fL_{bol}/h\nu$. A typical AGN continuum as parameterized by Mathews & Ferland (1987) yields $\nu \approx 9.96 \times 10^{15}$ Hz and $f \approx 0.54$.

2. The velocity field for the low-ionization line-emitting gas is mainly rotational. We assume that the velocity dispersion is the square root of the mean square velocity for a rotating annulus:

$$\sigma = \langle v^2 \rangle^{1/2} = \frac{1}{2\sqrt{2}} \sqrt{\frac{GM}{r}}\,, \qquad (3)$$

with FWHM($H\beta_{BC}$) = 2.35 σ.

We also consider the ratio I(Si III] λ1892)/I(C III] λ1909) to be a good density diagnostic (almost independent of the ionization parameter) in the density range $9.5 \lesssim \log n_e \lesssim 12$. CLOUDY (Ferland 2000) photoionization computations suggest that

$$\frac{I(\mathrm{Si\ III]\ }\lambda1892)}{I(\mathrm{C\ III]\ }\lambda1909)} \approx -3.91 + 0.41 \log n_e\,. \qquad (4)$$

Since the ratio I(Si III] λ1892)/I(C III] λ1909) is directly correlated with FWHM($H\beta_{BC}$) (Wills et al. 1999), adopting the FWHM($H\beta_{BC}$)-L/M correlation yields

$$\log n_e \approx 11.1 - 1.33 \log \mathrm{FWHM}_{1000}(H\beta)$$
$$\approx 7.72 + \tfrac{2}{3} \log (L_{bol}/M)_\odot\,. \qquad (5)$$

We can use equation (5) to write U in terms of L_{bol}/M:

$$U = 0.26(L_{bol}/M)^{-(1+x)}_{\odot,4} M^{-1}_{\odot,7}\,, \qquad (6)$$

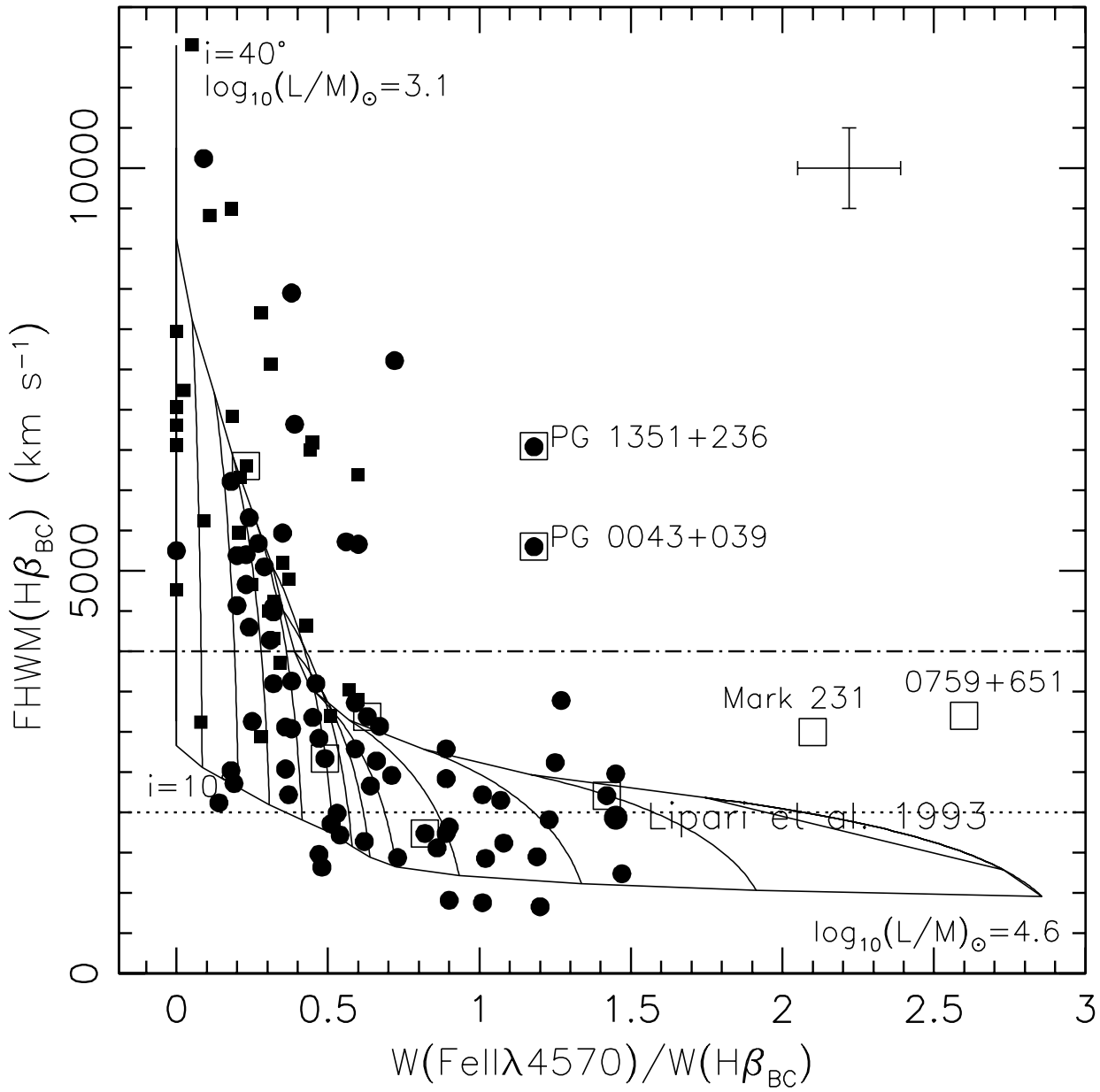

FIG. 4.—FWHM($H\beta_{BC}$) vs. $R_{Fe\,II}$ with a superposed grid of theoretical values as a function of i ($10° \le i \le 40°$) and L/M, expressed in solar values, for $3.1 \le \log (L/M)_\odot \le 4.5$ (implying $\log \dot{m} \approx 0$), at steps of $\log (L/M) = 0.1$. A value of $\log M \sim 8$ in solar units has been assumed for U. Data points are from Sulentic et al. (2000b). As in Fig. 3, filled circles represent RQ AGNs, and filled squares, RL AGNs. Data from Lipari et al. (1993) are shown as an average data point for objects clustering at $R_{Fe\,II} \approx 1.5$ and FWHM($H\beta_{BC}$) ~ 2000 km s^{-1}. Open squares mark BAL QSOs; they are traced around a filled circle if the object was present in the sample of Sulentic et al. (2000b). The horizontal lines mark the boundaries of NLSy1's (*dotted line*) and population A nuclei (*dot-dashed line*). The error bars in the upper right corner are typical 2 σ confidence level errors for a data point at FWHM($H\beta_{BC}$) ≈ 4000 km s^{-1} and $R_{Fe\,II} \approx 0.5$.

with $x = 0.67$, mass in units of $10^7\ M_\odot$, and the luminosity-to-mass ratio in units of 10^4 times the solar value [$(L/M)_\odot \approx 1.9$ ergs s^{-1} g^{-1}]. This accounts for the somewhat counterintuitive result that U decreases with decreasing FWHM($H\beta_{BC}$) and increasing L/M. We note that for $M_{\odot,7} = 1$ we obtain $\log U \approx -2$ for FWHM($H\beta_{BC}$) $\approx$ 2000 km s^{-1}, as expected. However, a shallower dependence may be possible; the L/M power is constrained within $1.1 \lesssim 1 + x \lesssim 1.7$ for a reasonable choice of the input parameters. For instance, if we use the relationship between luminosity and BLR radius $r_{BLR} \propto L^{0.7}$ (Kaspi et al. 2000), we would obtain $x \approx 0.1$. Values of $1 + x \gtrsim 1$ are a consequence of the assumption of a Keplerian (or virial or similar) velocity field (i.e., $v \propto 1/\sqrt{r}$).

5. CONNECTING THE OBSERVATIONAL PLANE TO L/M AND i

The above results allow us to relate L/M to the FWHM($H\beta_{BC}$)-$R_{Fe\,II}$ plane of E1. Determining the relationship between $R_{Fe\,II}$ and U is not trivial, since Fe II$_{opt}$ emission is poorly understood. Photoionization calculations suggest a fourfold increase in total Fe II$_{opt}$ emission from $\log U \approx -1$ to -2. We assume that $R_{Fe\,II}$ scales as total Fe II$_{opt}$ intensity divided by $I(H\beta_{BC})$ as a function of U for an average density $n_e \approx 10$ cm^{-3}. We use the calculations of Korista et al. (1997) to estimate the dependence on U. The normalization has been chosen following Blandford et al. (1990, p. 57), with $R_{Fe\,II} \approx 0.25$ for $\log U = -1$. We note

that using the possibly stronger correlation between I(Si III] λ1892)/I(C III] λ1909) and $R_{\rm Fe\,II}$ [i.e., I(Si III]λ1892)/I(C III]λ1909) $\approx 0.1 + 0.5\ R_{\rm Fe\,II}$; Wills et al. 1999] gives a consistent relationship without any assumption about the relationship between U and $R_{\rm Fe\,II}$. Equating the above relationship involving I(Si III] λ1892)/I(C III] λ1909) and $R_{\rm Fe\,II}$ to equation (4), and using equation (5) to relate n_e and L/M, allows us to obtain $R_{\rm Fe\,II} \propto 0.55 \log (L/M)$.

If low-ionization lines like Hβ are emitted in a flattened configuration, then some effect of viewing angle is expected. In order to take into account the effect of orientation, we assume the following:

1. The relationships employed above are valid for an average $i \approx 30°$. We write the FWHM(H$\beta_{\rm BC}$) dependence on i as

$$\mathrm{FWHM}(i) = \mathrm{FWHM}(0) + \Delta\mathrm{FWHM} \sin i\ , \qquad (7)$$

where

$$\Delta\mathrm{FWHM} = 2[\mathrm{FWHM}(i = 30°, L/M) - \mathrm{FWHM}(0)]\ . \qquad (8)$$

2. $R_{\rm Fe\,II}$ depends on i following a sec i law with a ratio $R_{\rm Fe\,II}$ that may change by a factor of 1.6 (an amplitude taken from the mean Fe II$_{\rm opt}$ difference between lobe-dominated and core-dominated RL objects).

These assumptions allow us to reproduce the parameter space covered by sources in our samples by assuming $\log M \sim 8$ in the expression of U and FWHM(0) = 500 km s^{-1}. Figure 4 shows a grid of theoretical values superposed on the data points of Sulentic et al. (2000a). If $1 + x < 1.7$ ($1 + x = 1.7$ is assumed in Fig. 4), then an $\dot{m}$ somewhat larger will result for the same $R_{\rm Fe\,II}$, yielding, however, the same qualitative behavior. For instance, for $x \approx 0.4$, $\log (L/M)_\odot \approx 4.5$ corresponds to $R_{\rm Fe\,II} \approx 1.5$.

6. DISCUSSION

Our calculations do not attempt to reproduce the observed point distribution but only to account for the occupancy of the parameter plane, since instrumental factors and biases affect the distribution. The cluster of points at $R_{\rm Fe\,II} \approx 0.2$, for example, is due to limits on the S/N and resolution. Another source of concern involves the role of selection biases in our E1 AGN sample. RQ population A sources are favored by selection techniques based on soft X-ray (e.g., Grupe et al. 1999) and optical color (e.g., BG92), while RL/RQ population B AGNs are not. The latter sources may be seriously underrepresented in the $R_{\rm Fe\,II}$ versus FWHM(H$\beta_{\rm BC}$) plane.

On the theoretical side, a distribution of masses will blur the grid, since different masses would deform and displace the grid horizontally. An additional source of scatter may involve Fe abundance. Therefore, no rigorous inference can be made about individual values of L/M and i from the Figure 4 grid.

The low-$R_{\rm Fe\,II}$ region ($R_{\rm Fe\,II} \lesssim 0.5$) of Figure 4 suggests that orientation is responsible for some of the population B sources. They would fall in the population A domain if viewed face-on. Toward the middle of Figure 4, we see that decreasing i and increasing L/M apparently have a concomitant effect [decreasing i implies decreasing FWHM(H$\beta_{\rm BC}$) and $R_{\rm Fe\,II}$; increasing L/M implies the same observational trends]. This is also true in the domain of NLSy1's, which should be an L/M extremum (but not necessarily of i). The concurrent effects of both parameters may explain why the correlations above have been found by a number of workers without any contradictory result. Observational prediction of some wind models are sensitive to both i and L/M and account, at least qualitatively, for the C IV λ1549 shift amplitude distribution as considered by Sulentic et al. (2000b).

Radiation pressure–driven wind models (Nicastro 2000; Witt et al. 1997) predict a decrease of $\dot{m}$ with increasing FWHM(H$\beta_{\rm BC}$). However, the model by Nicastro (2000) predicts highly super-Eddington accretion for NLSy1's. Existing evidence is still sparse, but neither a dynamical mass determination nor X-ray mass estimate supports this prediction. Rather, NLSy1's, as the bulk of population A sources, seem constrained within $0.3 \lesssim \dot{m} \lesssim 1.0$ (e.g., Puchnarewicz et al. 2001 constrain $0.3 \lesssim \dot{m} \lesssim 0.7$ for RE J1034+396; a similar result is inferred for Ark 564 by Comastri et al. 2001). Laor (2000a) also infers $\dot{m} \gtrsim 0.3$ for NLSy1's from X-ray variability. RQ AGNs with reverberation-mapping mass estimates (excluding NGC 4051 and NGC 4151) of Figure 3 show that there is no strong discontinuity between NLSy1 and the rest of population A [i.e., sources with 2000 km s^{-1} < FWHM(H$\beta_{\rm BC}$) $\leq$ 4000 km s^{-1}]. The $\dot{m}$-values become significantly different if population A and population B are compared with a Kolmogorov-Smirnov test (the difference is also appreciable in Fig. 3). The K-S test applied to population A (13 sources) and population B (11 sources) yields a probability $P \approx 1 \times 10^{-3}$ that the $\dot{m}$-values are drawn from the same parent population.

Most NLSy1 sources radiate at $\log \dot{m} \approx 0.0$, as do a sizable fraction of the sources with 2000 km s^{-1} < FWHM(H$\beta_{\rm BC}$) $\leq$ 4000 km s^{-1}, supporting the identification of a unique population up to at least FWHM(H$\beta_{\rm BC}$) $\approx$ 3500 km s^{-1}. PHL 1092 may be radiating at $\dot{m} \gtrsim 10$ (IRAS 13224−3809 may be another case). The extreme location of PHL 1092 in Figures 1 and 3 is consistent with both an exceptionally high value of $\dot{m}$ ($\gg 1$) and a pole-on orientation (also suggested by the strong X-ray variability; Forster & Halpern 1996). Sources like PHL 1092 may therefore be intrinsically rare even if not peculiar in a strict sense.

Recent results suggest a clear dichotomy between RL and RQ AGNs in terms of black hole mass, with RL AGNs having a systematically larger black hole mass (Laor 2000b). According to our considerations, the optical properties of AGNs should be largely transparent to black hole mass differences (with a dependence of U on M, yielding a second-order effect). However, the probability of having low L/M is obviously favored for large masses. This is in agreement with the upwardly displaced location of RL AGNs in the $R_{\rm Fe\,II}$-FWHM(H$\beta_{\rm BC}$) plot with respect to RQ AGNs. Also, in the idealized case of a sample where L is approximately constant, there could be a sequence of increasing mass from NLSy1 to population A and then to population B, with RL AGNs hosting the most massive black holes.

6.1. *On the Nature of the Outliers*

A major difference we are able to identify between the main sequence and outlying BAL QSOs is related to their far-IR spectral index α ($f_\nu \propto \nu^{-\alpha}$) between 25 and 60 μm. The

index $\alpha(25, 60)$ is 1.47 and 1.32 for Mrk 231 and 0759+651, respectively. Consistently, from ISO data (Haas et al. 2000), $\alpha(25, 60) \approx 1.13$ for PG 0043+039 (PG 1351+236 has been detected only at 60 μm). In both Figures 1 and 4, all the BAL QSOs known to us from Sulentic et al. (2000a) and Lipari et al. (1993) with $W(\text{C IV } \lambda 1549) \lesssim -9$ Å in absorption are reported. The three main-sequence BAL QSOs for which there are reliable *IRAS* or *Infrared Space Observatory* data (PG 1411+442, 1700+518, and 1001+054) have $\alpha(25, 60) \approx -0.24$, 0.56, and -0.33, respectively. In the remaining two cases (PG 1004+130 and PG 2112+059) it is not possible to compute the $\alpha(25, 60)$, but detection at 12 μm and no detection at 60 μm argues against large $\alpha(25, 60)$.

The most straightforward interpretation of this difference is a continuum steeply rising toward the far-IR because of a significant contribution from circumnuclear star formation in the outlying BAL QSOs (in line with the analysis of Haas et al. 2000 of the far-IR spectral shapes of PG quasars). This contribution may not be dominant in the main-sequence BAL QSOs. For both 0759+651 and Mrk 231, several lines of evidence suggest the presence of a strong circumnuclear starburst affecting the integrated broad-line spectrum of these AGNs (Taylor et al. 1999; Lipari 1994). If we consider the general population of AGNs in a diagram of rest-frame $W(\text{Fe II } \lambda 4570)$ versus $W(\text{H}\beta_{\text{BC}})$, we see that Fe II_{opt} strong quasars (their average is shown in Fig. 1; Lipari et al. 1993) define a boundary with $W(\text{Fe II } \lambda 4570) \approx W(\text{H}\beta_{\text{BC}})$, while the general population of AGNs fills the area with $W(\text{Fe II } \lambda 4570) < W(\text{H}\beta_{\text{BC}})$. Mrk 231 and 0759+651 remain outliers: they show $W(\text{Fe II } \lambda 4570)$ significantly larger than that expected from $W(\text{H}\beta_{\text{BC}})$. This may indicate a significant overproduction of Fe II_{opt} due to an additional excitation mechanism (i.e., shocks), possibly associated with strong circumnuclear star formation.

7. CONCLUSION

Our work (Sulentic et al. 2000a and references therein) shows that optical Fe II_{opt} emission is a fundamental parameter in AGN-correlation studies. This result underlies the need for more sophisticated models for the production of Fe II_{opt} (e.g., Verner et al. 1999). It also points out the need for much higher S/N spectroscopic observations of many sources with weaker Fe II_{opt} emission in order to clarify the upper left part of E1. In this paper we have attempted to explain, semiquantitatively but self-consistently, the diversity among RQ AGNs. Our attempt has been based upon the assumption that two of their most prominent emission features, $\text{H}\beta_{\text{BC}}$ and Fe II_{opt}, are influenced primarily by source orientation and the Eddington ratio. The results have allowed us to reinforce the distinction between two RQ AGN populations and to tentatively identify those AGNs that may be peculiar in a statistical and phenomenological sense, including some BAL QSOs.

The authors acknowledge fruitful discussion and encouragement from M.-H. Ulrich. M. C., P. M., and J. W. S. acknowledge support from the Italian Ministry of University and Scientific and Technological Research (MURST) through Cofin grants 98−02−32 and 00−02−004. T. Z. acknowledges support from the Slovene Ministry of Research and Technology.

REFERENCES

Blandford, R. D., Netzer, H., Woltjer, L., Courvoisier, T. J., & Mayor, M. 1990, Active Galactic Nuclei (Berlin: Springer)
Boller, T., Brandt, W. N., & Fink, H. 1996, A&A, 305, 53
Boroson, T. A., & Green, R. F. 1992, ApJS, 80, 109 (BG92)
Brandt, W. N., Laor, A., & Wills, B. J. 2000, ApJ, 528, 637
Brotherton, M. S. 1996, ApJS, 102, 1
Comastri, A., et al. 2001, A&A, 365, 400
Corbett, E. A., Robinson, A., Axon, D. J., & Hough, J. H. 2000, MNRAS, 311, 485
Corbin, M. R. 1997, ApJS, 113, 245
Czerny, B., Nikolajuk, M., Piasecki, M., & Kuraszkiewicz, J. 2001, MNRAS, 325, 865
Dultzin-Hacyan, D., Marziani, P., & Sulentic, J. W. 2000, in Astrophysical Plasmas: Codes, Models, and Observations, ed. J. Arthur, N. Brickhouse, & J. Franco (Rev. Mexicana Astron. Astrofis. Ser. Conf. 9) (México, D.F.: Inst. Astron., Univ. Nac. Autónoma México), 308
Falcke, H., Wilson, A. S., & Simpson, C. 1998, ApJ, 502, 199
Ferland, G. J. 2000, in Astrophysical Plasmas: Codes, Models, and Observations, ed. J. Arthur, N. Brickhouse, & J. Franco (Rev. Mexicana Astron. Astrofis. Ser. Conf. 9) (México, D.F.: Inst. Astron., Univ. Nac. Autónoma México), 153
Forster, K., & Halpern, J. P. 1996, ApJ, 468, 565
Gaskell, C. M. 1985, ApJ, 291, 112
Grupe, D., Beuermann, K., Mannheim, K., & Thomas, H.-C. 1999, A&A, 350, 805
Haas, M., Müller, S. A. H., Chini, R., Meisenheimer, K., Klaas, U., Lemke, D., Kreysa, E., & Camenzind, M. 2000, A&A, 354, 453
Kaspi, S., Smith, P. S., Netzer, H., Maoz, D., Jannuzi, B. T., & Giveon, U. 2000, ApJ, 533, 631
Korista, K., Baldwin, J., Ferland, G., & Verner, D. 1997, ApJS, 108, 401
Laor, A. 2000a, ApJ, 543, L111
Laor, A. 2000b, NewA Rev., 44, 503
Laor, A., Bahcall, J. N., Jannuzi, B. T., Schneider, D. P., & Green, R. F. 1995, ApJS, 99, 1
Laor, A., Bahcall, J. N., Jannuzi, B. T., Schneider, D. P., Green, R. F., & Hartig, G. F. 1994, ApJ, 420, 110
Lipari, S. 1994, ApJ, 436, 102
Lipari, S., Terlevich, R., & Macchetto, F. 1993, ApJ, 406, 451
Marziani, P., Sulentic, J. W., Dultzin-Hacyan, D., Calvani, M., & Moles, M. 1996, ApJS, 104, 37
Mathews, W. G., & Ferland, G. J. 1987, ApJ, 323, 456
Nicastro, F. 2000, ApJ, 530, L65
Pounds, K. A., Done, C., & Osborne, J. P. 1995, MNRAS, 277, L5
Press, W. H., Teukolsky, S. A., Vetterling, W. T., & Flannery, B. P. 1992, Numerical Recipes in Fortran (2d ed.; Cambridge: Cambridge Univ. Press)
Puchnarewicz, E. M., Mason, K. O., Siemiginowska, A., Fruscione, A., Comastri, A., Fiore, F., & Cagnoni, I. 2001, ApJ, 550, 644
Rodríguez-Pascual, P. M., Mas-Hesse, J. M., & Santos-Lleó, M. 1997, A&A, 327, 72
Sulentic, J. W., Marziani, P., & Dultzin-Hacyan, D. 2000a, ARA&A, 38, 521
Sulentic, J. W., Zwitter, T., Marziani, P., & Dultzin-Hacyan, D. 2000b, ApJ, 536, L5
Taylor, G. B., Silver, C. S., Ulvestad, J. S., & Carilli, C. L. 1999, ApJ, 519, 185
Ulrich, M., Maraschi, L., & Urry, C. M. 1997, ARA&A, 35, 445
Verner, E. M., Verner, D. A., Korista, K. T., Ferguson, J. W., Hamann, F., & Ferland, G. J. 1999, ApJS, 120, 101
Wills, B. J., Laor, A., Brotherton, M. S., Wills, D., Wilkes, B. J., Ferland, G. J., & Shang, Z. 1999, ApJ, 515, L53
Witt, H. J., Czerny, B., & Życki, P. T. 1997, MNRAS, 286, 848